ISAC Beam Energy Measurement using DRAGON MD1

D.A. Hutcheon

December 20, 2002

1 Introduction

The dispersed focus following DRAGON's magnetic dipole MD1 can be used to measure the energy of beams delivered by the ISAC accelerators. This note summarizes the properties of the DRAGON system and discusses the sources of error in the energy measurements.

2 Ion optics: dispersion and magnification

DRAGON quadrupoles Q1 and Q2 and dipole MD1 produce at the Charge slits an image of the beamspot at the centre of the gas target. In the horizontal (x) direction the magnification is -0.44. This is an energy-dispersed focus, the position at slit XSLITC varying by 0.30 cm per 1% change in beam energy relative to a "central" energy.

The way energies have been measured on MD1 is to vary the magnetic fields until the beam is centred at x=0 at the Charge slits. In this way, the determination of beam energy does not hinge on exact knowledge of the dispersion of the QQD system.

However, the dispersion, D, and the magnification, M, are important in setting the **sensitivity**, the uncertainty in a beam energy measurement. An error δx_c in the user's centring of beam to x=0 at the charge slit focus will result in an error $\delta x/M$ in the computed beam energy; if the beam is off-axis at the gas target by δx_t, the resulting error in energy is $\delta x_t \cdot M/D$.

The first-order focus condition ensures that the beam position at the Charge slit is independent of the beam direction through the gas target. The calculated second-order effect is -15μm/(mrad)^2: the tubes of the gas target differential pumping stages limit beam direction to within 3–4 mrad of the ion-optic axis, meaning the error in beam energy would be at worst

$$-15 \times 4^2/(10000 \times 0.30) = 0.08\%$$

Normal tuning procedures ensure a much smaller error from this source.

The second-order term proportional to the square of fractional energy deviation is -21μm/(%)^2. Although magnets are tuned to make the central energy the same as the median (or mean) beam energy, the RMS energy spreads are typically 0.75–1.2 keV/u, which for a 200 keV/u beam is a fractional variation of 0.38–0.6%. The shift in beam position at the Charge slits due to energy spread should be not worse than

$$-21 \times 0.6^2 = 7.5\mu m$$

which can be neglected in comparison to other effects.

In the situation where uncertainty in beam energy comes mainly from the beamspot size, the figure of merit of the spectrometer is the ratio D/M. The Prague magnet, with its 90° bend, has a D/M more than twice that of MD1. Clearly, it is the device of choice for measuring beam energy spread.

3 Random errors of the method

3.1 "Theory"

The standard measurement method is to close slits XSLITC until a substantial fraction of beam is intercepted, then adjust the magnet fields until equal beam currents are measured on the Left and Right slits. Because the slits have no electron suppression, it is not guaranteed that equal slit currents mean equal amounts of intercepted beam. (The secondary electron emission coefficients could be different for the two slits.) The alternate method of scanning the slits and measuring current transmitted to the Faraday cup is much slower and requires that the beam intensity remains constant.

Disregarding the question of secondary electron emission, there remains the question: what is the "energy" of the beam when the energy distribution is asymmetric? Two obvious definitions are the mean beam energy or the median beam energy. The method of putting equal amounts of beam on Left and Right slits measures the median energy in the limit where all the beam is intercepted. Real measurements obtain something different, typically something like "the average of the energies at the 15-percentile and the 85-percentile". If the best possible energy measurement is needed for a beam of asymmetric energy distribution, it will be necessary to record the distribution (Prague magnet harp monitor) and also the fraction of beam let through to the Faraday cup when the slit currents are balanced.

The optimum slit width is a balance between the problems due to possible asymmetry in energy distribution *vs* electron emission factors. If we were dealing with a Gaussian distribution in x and were intercepting 15% of the beam on each slit, a displacement of the entire peak by 0.1σ will produce a Left-Right difference which is 5% of the total beam current. Clearly, the sensitivity depends on the ratio of beam current to electronic noise.

To make a rough estimate of the random error of measurement associated with the centring of the beam on the slits, take $\sigma_x = 1$ mm and assume the "centre" can be defined to $0.1\sigma = 0.1$mm. This corresponds to a beam energy error of $0.1/3 = 0.03\%$, to be expected when total beam intensity is of order $10/0.05 = 200$ epA. At this level (100 μm) we must question also whether the slit drive gives consistent positioning.

3.2 "Experience"

The following tables record the beam energies deduced "no gas" and "with gas" for three excitation function studies. The differences should be constant (or, at most, slightly varying with energy) and can be used to assess the consistency of MD1 energy measurements.

The RMS spread in energy differences on Table 1 is 0.74 keV/c, or 0.52 keV/c = 0.07% per energy measurement. If run 6920 is excluded, the RMS variation is 0.025% (equivalent to 75μm in x).

In Table 2 the selected charge state was 6+, except for run 6901 where it was 7+ and 6909 where it was 5+. The RMS variation in energy difference is 1.46 keV/c or 0.2% per energy measurement.

Table 3 had RMS energy difference spread of 0.56 keV/u, excluding run 6858. This corresponds to $\sigma = 0.18\%$ per energy measurement.

There was no record of the beamspot sizes, but we would expect the higher energy beams to have smaller transverse emittance. The beam energy spreads were recorded at the Prague magnet: typically the two series around 520 and 760 keV/u had energy spreads of 0.2% FWHM, while at 220 keV/u they were 0.5%.

It is not clear how to view the results at 760 keV/u. Either they were approaching the level of consistency expected under ideal conditions and run 6920 was an "oops", or it just happened that 15 out of 16 runs clustered very close to each other.

Gas/No-gas differences do not have a contribution due to variation in beam position at the gas target. In early measurements there was no direct control over the beam

Table 1: Beam energy measurements, ^{21}Ne in H_2.

Run	E(No gas) keV/c	E(Gas) keV/c	ΔE keV/c	Pressure Torr
6911	778.0	762.9	15.1	4.60
6912	775.4	759.9	15.5	4.56
6913	772.0	756.3	15.7	4.57
6914	769.1	754.1	15.0	4.56
6915	766.1	750.9	15.2	4.57
6920	762.3	749.9	12.4	4.57
6923	760.2	745.0	15.2	4.59
6924	755.9	741.0	14.9	N/A
6925	752.5	737.8	14.7	4.59
6926	764.4	749.1	15.3	4.59
6927	763.5	748.7	14.8	4.57
6928	761.0	745.8	15.2	4.59
6930	772.8	757.8	15.0	4.59
6931	787.0	771.5	15.5	4.56
6932	768.8	753.7	15.1	4.59
6938	771.0	755.9	15.1	4.40

Table 2: Beam energy measurements, ^{21}Ne in H_2.

Run	E(No gas) keV/c	E(Gas) keV/c	ΔE keV/c	Pressure Torr
6897	514.4	507.3	7.1	3.00
6898	516.7	507.5	9.2	3.00
6899	521.3	511.1	10.2	3.00
6900	523.6	513.6	10.0	3.06
6901	525.3	514.8	10.5	3.09
6902	525.3	518.7	6.6	–
6905	526.8	517.1	9.7	3.07
6907	516.0	505.3	10.7	3.11
6909	524.9	512.0	12.9	4.26
			[9.4]	[3.11]

Table 3: Beam energy measurements, ^{24}Mg in H_2.

Run	E(No gas) keV/c	E(Gas) keV/c	ΔE keV/c	Pressure Torr
6881	225.65	213.24	12.41	4.52
6883	226.31	213.83	12.48	4.53
6832	228.4	216.0	12.4	4.5
6835	224.3	212.5	11.8	4.5
6840	223.7	210.3	13.4	4.64
6841	228.6	215.6	13.0	4.61
6851	236.1	223.0	13.1	4.51
6857	223.7	211.0	13.7	4.49
6858	223.7	219.8	3.9	1.48
6861	220.4	208.4	12.0	4.5
6864	219.85	207.48	12.37	4.61
6874	222.85	209.92	12.93	4.64
6876	221.8	209.4	12.5	4.5

position, indirect control by maximizing transmission. Recent (fall 2002) measurements have generally included a check on beam position; future measurements should be able to use a CCD image for better control of beamspot position at the gas target.

4 Systematic errors

4.1 Kinematics

On-line estimates of E/M, beam energy per unit mass, from the MD1 magnetic field B typically make a non-relativistic approximation. The relativistic expression gives E/M that is smaller by

$$[1 - (1/2)(E/Mc^2) + ...]$$

which amounts to a correction of 0.08/A% for E/M = 1.5 MeV/u.

Ignoring the mass of the electrons stripped from the atom typically is an error of

Table 4: MD1 magnetic field as a function of setpoint current. Data taken from Hardware logbook, page 58 (4 Sept 2002).

Current I (Amp)	Field B (Gauss)	B/I (Gauss/Amp)	(B-100)/I (Gauss/Amp
250	3030.0	12.120	11.720
275	3324.6	12.089	11.726
300	3618.5	12.062	11.728
325	3912.9	12.040	11.732
350	4206.5	12.019	11.733
375	4499.6	12.000	11.732
400	4792.1	11.980	11.730
425	5083.6	11.943	11.726
450	5374.4	11.943	11.721
250	3031.3	12.125	11.725

0.02% per electron and rounding of atomic masses (e.g. 21 for 20.994) is similar in magnitude (except for the proton, 1.0073 amu).

These corrections are all negligible on the scale of precision which can be achieved with ISAC + DRAGON. The relativistic correction and correction for stripped electrons will be ignored in what follows.

4.2 B vs I in MD1

The B-vs-I data have two noteworthy features. First, the deviation from linearity is small and regular, about -0.4% per kG, as might be due to an approach to saturation in steel at the corners of the yoke, for example. (Alternatively, as suggested by the empirical formula of the right-hand column, a zero offset in the current transducer could account for most of the observed non-linearity in B/I.) Second, hysteresis is small (at least at the position of the NMR probe.

Table 5: MD1 magnetic field as a function of selected charge. Beam was ^{24}Mg at 228 kev/u.

Charge q	Field B (Gauss)	q*B (Gauss)
3	5360.05	16080
4	4016.37	16065
5	3212.14	16061
6	2675.86	16055

4.3 Field vs charge state

In DRAGON logbook #8, page 152 are data from measurement of beam energy using different charge states of a 228 keV/u ^{24}Mg beam, reproduced in Table 5.

There is a monotonic increase in qB as B increases and q decreases, amounting to about 0.06% per kG. Two possibilities present themselves:

- magnet saturation effects which affect the site of the NMR probe less than they do the field integral experienced by the beam ions. It is not implausible that *differential* saturation might be an order of magnitude smaller than the modest saturation seen in the B-vs-I data.

- different average energy losses in the target for ions that exit in different charge states. Clearly, an ion which emerges in q=6 has had a higher average charge in the gas target than an ion emerging in q=3, and it is plausible that higher q means higher dE/dx. The difference between the q=3 and q=6 cases corresponds to a difference in energy loss which is about 2% of the total loss in passing through the gas.

It will not be easy to distinguish these two possibilities. The field maps at 485 A and 295 A show a ratio of field integral divided by field at the NMR probe site which changed by only 0.06%. It is difficult to assess the uncertainty in these measurements because MD1 is not rectangular, making the field integral sensitive to “x” position. The energy-loss theory is hard to test, also.

4.4 Absolute scale: calculated E/A vs B

The ion-optical design of DRAGON called for a central trajectory with radius of curvature ρ=1.0 m through MD1. The momentum of the ion, p, the uniform magnetic field, B, and the ion charge, q, are related by

$$p = Bq\rho$$

in MKS units. If we express p in MeV/c, q in units of the electron charge, ion energy E in MeV and ion mass A in atomic mass units (u=931.49$\times 10^6$ eV/c^2), the non-relativistic expression becomes

$$E = \frac{1}{2M}p^2 = \frac{1}{2Au}(Bq\rho)^2$$

or

$$E/A = (\frac{c^2}{2uc^2}\rho^2)(Bq/A)^2$$

With ρ=1.0 m the constant becomes

$$299792458^2/(2 \times 931.49 \times 10^6) = 4.824 \times 10^7 eV/u$$

4.5 Absolute scale: B measured for (p,γ) resonances

A number of methods have been used to relate quantities measured by DRAGON to radiative capture resonance energies obtained from the literature:

- E(z=0) as P$\to$0. Recoil-gamma coincidence data are taken at several beam energies and gas target pressure, the mean z position of the detecting BGO’s being calculated in each case. At a given pressure the beam energies are chosen to give two z values close to and bracketing z=0. The interpolation of z at each pressure and extrapolation to P=0 gives the resonance energy. The advantage is that both the gas density profile and BGO efficiency are in their "flat" region at all times. The method is limited by the statistics of calculating z and the single-run uncertainty in measuring beam energy with MD1 (0.2%).

- E at $Y(E)=\frac{1}{2}Y_{max}$. Target pressure is held constant and the beam energy scanned through the low-energy edge of the thick-target yield curve. The energy at which the yield is 50% of the maximum yield is where the median beam energy matches the resonance energy. Only modest statistics are required. The single-run uncertainty in measuring energy with MD1 (0.2%) combined with the steepness of slope (due to beam energy spread) defines the ability to find the half-height energy. A problem with this method is that the resonance is being shifted upstream out of the gas cell and into a region where gas density and BGO efficiency are dropping rapidly. From my analysis of target studies (notes of June 3, 2002), a plausible estimate is that 2±1% of the gas is at the upstream half of the first upstream pumping tube and "out of sight" of the detectors.

- E + ΔE(z). Recoil-gamma coincidence data are taken at a single beam energy and gas pressure such that the resonance is situated near z=0. The beam energy is measured without and with gas in the target, and the fraction of energy loss to reach z, ΔE(z) is subtracted from the no-gas energy E (or the calculated energy loss from z through the rest of the target is added to the with-gas energy). This method requires only one energy setting. The resonance is located where gas density and BGO efficiency *vs* z is flat. As always, the MD1 measurement uncertainty (0.2%) is present. The calculation of $\Delta E(z)$ has an uncertainty due to statistics of computing z plus the systematic uncertainty in the slope d(E/M)/dz.

- "Zero-crossing" of the elastic scattering cross section. In the few cases where the resonance is strong enough to cause deviation of the Elastic Monitor rate from pure Coulomb scattering, the resonance energy can be deduced from the shape of the curve of normalized rate *vs* beam energy. The Elastic Monitor views always the same volume of gas slightly upstream of the centre of the cell: beam energy loss to that point must be calculated. The single-run uncertainty from MD1 and the resonance width are limits to the precision of this method.

Table 6 shows results from measurements of a number of resonances, either where energy calibration was the primary purpose of the runs or where it was a useful by-product. Table 7 gives values from the literature or from compilations and compares the DRAGON results with them. The differences are plotted in Figure 1 as a function of E/M of the beam.

The sensitivity to analysis method my be gauged by comparison of the ^{24}Mg result obtained here by interpolating two points near half-maximum yield (222.3 keV/u) with Sabine Engel's fit to an analytic yield-curve function (221.8 keV/u). The difference is about the size of the quoted uncertainties.

Of the data presented in Figure 1, those at 270 keV/u and 1160 keV/u should be the most reliable: the literature values seem to be well-determined with uncertainties much smaller than we could hope to see, and our "extrapolation to zero pressure" method keeps the resonance in the central part of the gas cell. Next in line should be the low-energy ^{24}Mg point, again with a precise literature value. The ^{24}Mg point at 817 keV/u and ^{21}Ne point at 762 keV/u were by-products of other measurements;

Table 6: Resonance energies measured on DRAGON. A 4-digit Reference indicates the relevant MIDAS run number, roman–arabic Reference indicates the DRAGON logbook number–page.

Reaction	Method	Reference	B(MD1) (Gauss)	E_{beam} (keV/u)	ΔE(z) (keV/u)	E_{res} (keV/u)
^{24}Mg(p,γ)	E at Y=0.5Y_{max}	6874/6876	2714	222.4±0.4	-0.2±0.1	222.3±0.4
	E - ΔE(z)	5268	5225.2	824.2±1.6	-8±2	816±2.5
^{21}Ne(p,γ)	E(z=0) as P→0	S. Engel	3927.4±3.1	270.1±0.4	0	270.1±0.4
	E at Y=0.5Y_{max}	6896-7/6906	4345.6	516.7±0.1.0	-0.2±0.1	516.5±1.0
	E - ΔE(z)	7229	3270.9	749.4±1.5	+10.8±1.1	760.2±1.9
	Elastics	6914/6926	5287/5303	767.2±1.5	-6.3±1	761.0±1.8
^{20}Ne(p,γ)	E(z=0) at P→0	S. Engel	3874.0±0.7	1158.6±0.4	0	1158.6±0.4
^{14}N(α,γ)	E - ΔE(z)	IX–49	2472.2	375.9±0.8	+4.8±1.2	380.7±1.5

Table 7: Resonance energies from the literature compared with DRAGON measurements.

Reaction	Reference	E_{beam} (keV)	$(E/M)_{lit}$ (keV/u)	DRAGON-Literature Difference (%)
^{24}Mg(p,γ)	Uhrmacher	222.89±0.08	221.28±0.08	+0.46±0.18
	Endt78	823.1±0.5	817.2±0.5	-0.15±0.31
^{21}Ne(p,γ)	Becker92	271.54±0.04	269.58±0.04	+0.19±0.15
	Endt78	524.7±1.5	520.9±1.5	-0.84±0.35
	Endt78	767.9±0.5	762.4±0.5	-0.29±0.26
				-0.18±0.25
^{20}Ne(p,γ)	Endt78	1168.8±0.4	1160.4±0.4	-0.17±0.05
^{14}N(α,γ)	Tilley95	1529±2	382.1±0.5	-0.37±0.41

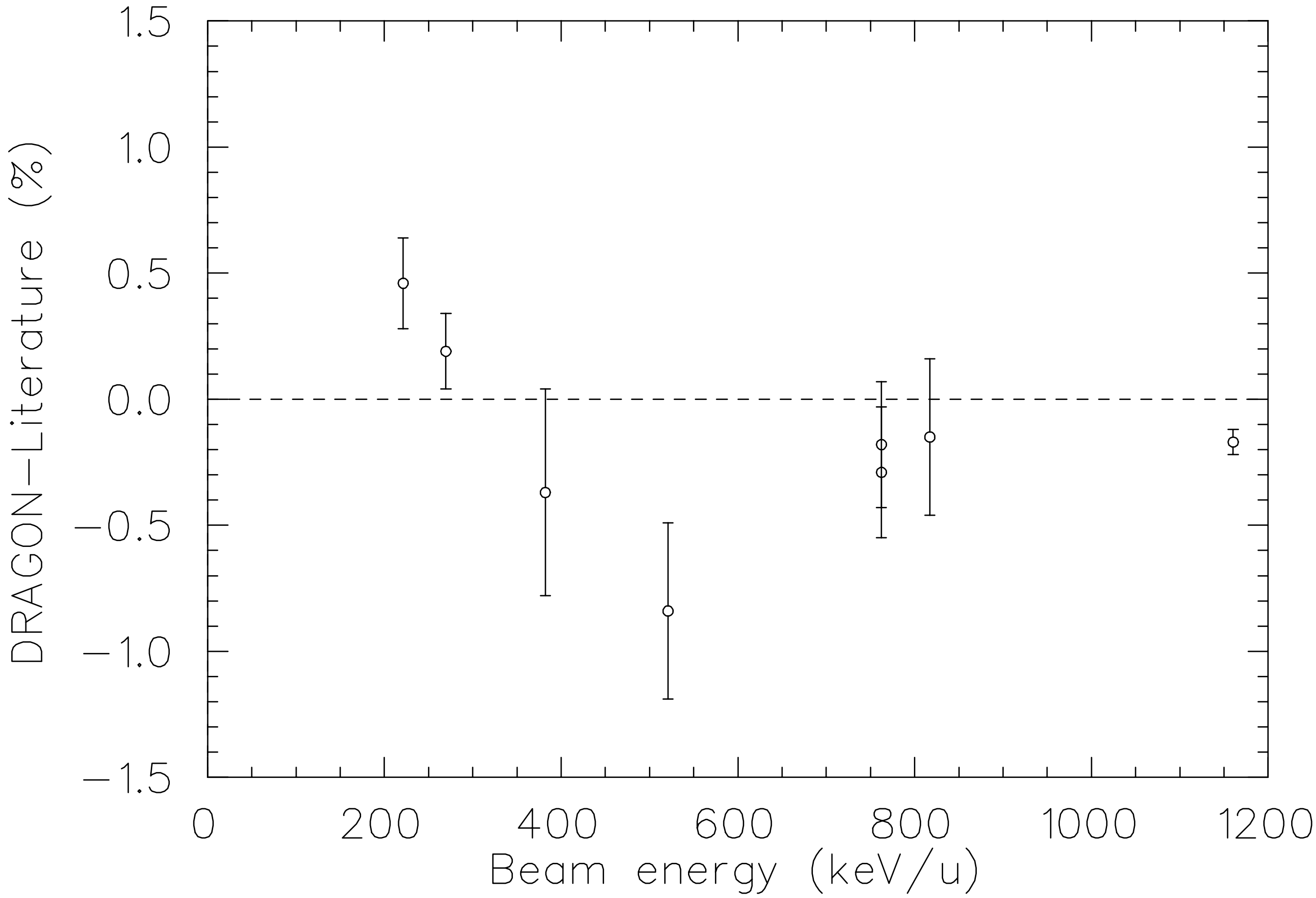

Figure 1: Beam Energy/amu for selected resonances: differences between DRAGON and literature values.

the ^{14}N 382 keV/u point was taken in a half-hour before a maintenance day and had substantial background in the coincidence spectrum. The Elastic Scattering resonance method does not show to its full potential because of the unfortunate loss of data from two key runs, leaving a gap of 5 keV/u between runs 6914 and 6926.

The black sheep of the family is the ^{21}Ne resonance at "520.9" keV/u. The discrepancy was observed twice, in scans taken two months apart with different recoil detectors. The weaker resonance at "500.1" keV/u is seen by us, also about 1% lower in energy than the literature value. It turns out that the literature consists of a single experiment (Antilla *et al.*, Z.Phys. **234**(1970)455) which used an implanted target and measured resonances from 0.5 to 1.29 MeV proton beam energy. Unfortunately, their range did not extend down to cover the resonance at 270 keV/u. Later experiments with gas targets (Berg et al., Gorres et al.) used the quoted energies of Antilla et al. as calibration points, so there is no independent confirmation of the early result.

5 Conclusions

- The scale uncertainty in calculating beam energy from MD1 field is about 0.2%, based on calibration using established (p,γ) resonance energies. The calibration constant computed for the nominal MD1 bending radius, 48240 (keV/u)/(Tesla/u)^2, is very close to the best-fit value.

- The random (non-statistical) error in making one measurement of beam energy is about 0.2%, based on scatter in Gas-NoGas differences. There is an indication that under some conditions the RMS scatter can be smaller by a factor of $\approx$3.

- Over a 2:1 range in magnetic fields, the product of MD1 field times selected charge changes by 0.15%. It is not clear whether this is a change in the MD1 effective length with field, or whether it is due to slight variation in beam energy loss according to the charge state at exit.

- DRAGON results suggest that two resonances in ^{21}Ne(p,γ) lie 4–5 keV/u lower in energy than the literature value.